Optical pumping dynamics and near-resonance light scattering in an ultracold sample of ^{87}Rb atoms

S. Balik and M. D. Havey*
Department of Physics, Old Dominion University, Norfolk, Virginia 23529, USA

I. M. Sokolov and D. V. Kupriyanov†
Department of Theoretical Physics, State Polytechnic University, 195251 St. Petersburg, Russia

(Received 18 December 2008; published 30 March 2009)

We report measurements of near-resonance light scattering from an ultracold sample of ^{87}Rb atoms formed in a magneto-optical trap (MOT). Time-dependent measurements of scattering of probe radiation tuned in the vicinity of the $F=1\rightarrow F'=0$ hyperfine transition of the D_2 resonance line reveal dynamics due to Zeeman optical pumping on this transition in competition with diffusive light scattering in the optically dense sample. Zeeman mixing effects due to small residual magnetic fields also play an important role in the scattered light dynamics and reveal surprising sensitivity to the field strength. The various processes are examined as a function of probe-laser power, detuning from atomic resonance, and the presence or absence of the spatially inhomogeneous MOT quadrupole field.

DOI: 10.1103/PhysRevA.79.033418 PACS number(s): 34.50.Rk, 34.80.Qb, 42.50.Ct, 03.67.Mn

I. INTRODUCTION

Studies of dynamical processes involving ultracold atoms is a broad and vigorous area of research in atomic physics. Experimental techniques developed in part to pursue quantum degeneracy of composite bosonic atoms [1] have found a constellation of new applications [2–6] and led to rich insights, in such scientific research areas as quantum optics, molecular physics, precision measurements, and discoveries at the boundaries between atomic and condensed-matter physics. One such specialized area of current research in quantum optics concerns the exploration of the role of disorder in atomic and photonic wave scattering [7–11]. Among current research topics are experimental and theoretical efforts in the area of random lasing in an ultracold atomic gas [12]. Such effects are a significant area of research in condensed-matter and materials physics [9], and ultracold atomic physics studies may lead to insights and to new gain mechanisms for such processes. Another area of considerable interest is the possibility of light localization by disorder in an ultracold atomic gas of sufficient density. Such studies are the natural progeny of original studies of electron localization by Anderson [7] but directed to photonic studies in later proposals [13,14]. There exists a quite large literature of such researches in photonic materials and in disordered condensed samples [15–21], but atomic physics studies so far remain limited in comparison [22–26]. One reason for this is that the canonical condition guiding the search for localization, the Ioffe-Regel criterion, puts high demands on the required atomic density. This condition is $kl\sim 1$, where k is the magnitude of the wave vector and l is the transport mean-free path [27]; an atomic density $\sim 10^{14}$ atoms/cm^3 seems necessary.

We have a research effort to search for the light localization in an ultracold and high-density sample of ^{87}Rb atoms. This sample is formed initially in a magneto-optical trap (MOT) and then compressed to much higher density in a far-off-resonance optical dipole trap [28]. As a prelude to those studies, we have investigated the time dependence of light scattering from lower density yet optically thick samples for which the competing roles of Zeeman optical pumping and diffuse light scattering needed to be disentangled. Optical pumping plays an important role for the $F=1\rightarrow F'=0$ hyperfine transition of the D_2 resonance line, for any unidirectional and polarized probe will optically deplete one or more of the Zeeman sublevels of the $F=1$ level. This effect dynamically and significantly reduces the optical depth of the sample as a whole.

In this paper, we report experimental studies of light scattering in the spectral vicinity of the D_2-line $F=1\rightarrow F'=0$ hyperfine transition in ^{87}Rb. We find strong variations in the time dependence of the scattered light intensity as a function of the probe-laser detuning from resonance and as a function of the intensity of the probe laser itself. In addition to this, we find that a small residual magnetic field present at the sample site during the measurements can have a strong effect on the results. Depletion of the optically pumped Zeeman substate [29,30] makes the sample quite sensitive to residual fields and effects of average magnetic fields on the order of 50 μG are readily observable.

In Secs. II–IV we first present a description of the experimental apparatus, sample characteristics, and experimental approach. This is followed by the discussion of measurements of the light-scattering dynamics with the trap magnetic field both on and off and of measurements of the magnetic field transients taking place when the field is turned off during the measurement cycle. We conclude with a summary of our main results and their context.

II. EXPERIMENTAL DETAILS AND PROTOCOLS

A diagram of the layout of the instrumentation used in the measurements is shown in Fig. 1, while a schematic energy-

*mhavey@odu.edu
†Kupr@DK11578.spb.edu

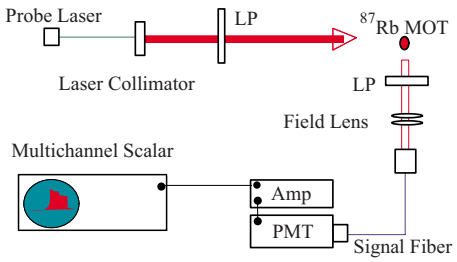

FIG. 1. (Color online) Schematic diagram of the experimental apparatus. In the figure, LP refers to a linear polarization analyzer, Amp refers to a fast preamplifier, while PMT indicates a photomultiplier tube.

level diagram for the pertinent hyperfine levels of ^{87}Rb is shown in Fig. 2. As seen in Fig. 1, the central part of the experimental apparatus is a MOT confining ultracold ^{87}Rb atoms. The MOT is a standard vapor-loaded trap formed in a vacuum chamber with a base pressure $\sim 10^{-9}$ Torr. The six MOT beams are derived from a single diode laser operated in an external cavity formed by the diode back facet and a grating arranged in a Littrow configuration. By measurement of the spectral noise measured by heterodyne comparison (at 10 MHz offset) of the spectral noise generated by two lasers of nearly identical design, the full spectral width of the MOT and repumper lasers was estimated to be less than 1 MHz. The main diode laser power is amplified by an injection-locked slave laser; the entire setup providing about 20 mW of trapping light in laser beams of cross-sectional area ~ 2 cm^2. The master laser is locked to a saturation absorption feature produced in a room-temperature Rb vapor cell. The main trap laser is switched and spectrally shifted as required with an acousto-optical modulator (AOM) to a frequency set at about 18 MHz below the ^{87}Rb $F=2 \rightarrow F'=3$ trapping transition, viz., Fig. 2. The required repumper laser is of the same basic design as the main MOT laser but is of sufficient power that no slave laser is necessary. As for the master laser, the saturated absorption in a room-temperature Rb vapor cell is used to lock the repumper to the $F=1 \rightarrow F'=2$ transition. The repumper delivers a beam of maximum intensity ~ 0.6 mW/cm^2 to the trap area. An AOM is

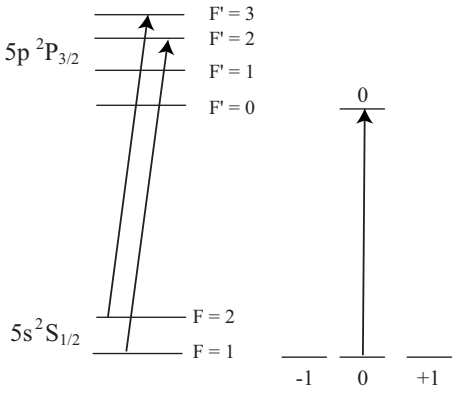

FIG. 2. Schematic energy-level diagram for relevant hyperfine and electronic levels in ^{87}Rb. The Zeeman sublevels of the $F=1 \rightarrow F'=0$ hyperfine transition are broken out on the right side of the figure.

used to control the application of the repumper beam to the ultracold sample. We point out that the loading time for the trap is about 3 s. However, in the experimental protocol, the duty cycle for the each measurement is about 100 ms; this means that the majority of the atoms are regathered into the trap after each measurement with little loss in the overall signal.

In the experiments reported here, measurements are made on atoms in the lower-energy $F=1$ hyperfine level. The cold atom sample is initially produced in the higher-energy $F=2$ level, and direct absorption imaging measurements of the peak optical depth on this transition yielded $b_0 \sim 10$. In order to transfer these atoms to the lower-energy hyperfine component, the repumper laser is switched off while leaving the MOT lasers on. Leaving the MOT trap lasers on allows for weak optical pumping through far-off resonance (from the $F=2 \rightarrow F'=2$ $F=2 \rightarrow F'=1$ transitions; see Fig. 2) inelastic Raman transitions to the lower-energy $F=1$ hyperfine level. In about 1 ms, this transfers nearly all the atoms in the upper $F=2$ hyperfine ground level component to the desired $F=1$ hyperfine component. This was experimentally confirmed by reflashing the MOT lasers, but not the repumper laser, for a brief period and measuring the resulting fluorescence signal. This was found to be negligible in comparison with similar measurements done before the optical pumping process, implying a transfer efficiency from the $F=2$ to the $F=1$ ground hyperfine level greater than 99%.

In the present experiments, the atomic sample is quite well described by a Gaussian atom distribution at a temperature T. For such a sample, the spherically symmetric spatial distribution of atoms $n(r)$ is given by

$$n(r) = n_0 e^{-r^2/2r_o^2}, \tag{2.1}$$

where the Gaussian radius is r_0 and the peak number density at the center of the trap $(r=0)$ is n_o. The total number of atoms in the trap N is given by

$$N = (2\pi)^{3/2} n_0 r_0^3, \tag{2.2}$$

and the peak optical depth is

$$b_0 = \sqrt{2\pi} n_0 \sigma_0 r_0. \tag{2.3}$$

Here σ_0 is the weak-field resonance light-scattering cross section.

The important sample characteristics are those associated with the atoms in the lower-energy $F=1$ hyperfine level. These characteristics, including the total number of atoms in the trap, are determined by measurements of the spectral dependence of the optical depth and the spatial dimensions of the ultracold atomic cloud. We describe in Sec. III B how we determine the peak optical depth through fluorescence measurements, for which we obtain a peak optical depth of $b_0=3.5(5)$ for the ^{87}Rb $F=1 \rightarrow F'=0$ transition after the optical pumping phase. Note that because of the larger light-scattering cross section, this implies a peak optical depth 4.2 times larger on the $F=2 \rightarrow F'=3$; this result is consistent with our earlier measurements with this system. With a Gaussian radius measured by the fluorescence imaging of the sample $r_o \sim 0.45$ mm, we obtain the total number of atoms

in the trap (and hence in the lower hyperfine level) $N \sim 10^8$. The sample temperature was determined through measurements of the ballistic expansion of the sample to be ~ 100 μK.

To make time-dependent fluorescence measurements on the ultracold sample, the atomic cloud is excited by a linearly polarized probe beam tuned in the spectral range of $\pm 2\gamma$ around the $F=1 \rightarrow F'=0$ hyperfine transition of the ^{87}Rb D_2 resonance line. Here we use $\gamma=5.9$ MHz for the natural width of the transition [31]. We define a detuning δ for the probe laser as $\delta=f_p-f_{10}$, where f_p is the probe-laser frequency and f_{10} is the resonance frequency of the $F=1 \rightarrow F'=0$ transition. For all data, the fluorescence is viewed at right angles to the probe **k** vector. Selecting the quantization axis for the system to be along the linear polarization direction of the probe beam, the selection rule for allowed Zeeman transitions is $\Delta m_f=0$. The probe-excited scattered light intensity is generally collected without regard for the polarization state and focused into a multimode fiber which delivers the photon signal to a cooled GaAs photomultiplier tube operated in a photon counting mode. When the polarization assessment of the fluorescence was made, a linear polarization analyzer was inserted in the fluorescence detection channel, as shown in Fig. 1. The photon counting pulses are amplified, time sorted, and stored in a multichannel scalar, which is set up so that the time bins in the present experiments are 40 ns. The overall collection efficiency of the detection system is estimated to be about 0.1%. Signals due to background and scattered light are found to be completely negligible compared to the fluorescence signals of interest. Finally, although the scattered light in the spectral vicinity of the studied $F=1 \rightarrow F'=0$ transition is expected to be unpolarized, an auxiliary polarization diagnostic setup in the fluorescence detection arm was used from time to time to confirm this.

III. RESULTS AND DISCUSSION

A. Fluorescence measurements: Trap magnetic fields off

In this section we report fluorescence measurements done while the MOT quadrupole fields are turned off. To ensure that the fields are small, the field current is turned off about 4 ms before the measurement cycle begins. We will see in Sec. III B that effects due to the transient field are not entirely negligible even after this quite long time delay. In general, nearly all measurements reported here are made for a single linear polarization of the fluorescence channel. Weak-field light scattered on the $F=1 \rightarrow F'=0$ hyperfine transition is necessarily unpolarized. However, the $F=1 \rightarrow F'=1$ hyperfine transition is energetically located 72.3 MHz to higher frequencies than the $F=1 \rightarrow F'=0$ transition. Therefore, there can be small contributions to the measured signals in the detuning range we study here. These depend on detuning and are about 10% at the largest detunings we used in these experiments. For the transient measurements reported below, these contributions are typically on the order of 2% or less and are neglected in our discussions. We should also point out that these parasitic contributions are in general linearly polarized, with a polarization degree of about 20% we checked for possible linear polarization of the fluorescence signal for a range of conditions. Within the few percent accuracy of these measurements, no linear polarization of the fluorescence was found. At frequencies much closer to the $F=1 \rightarrow F'=1$ transition than were used in these experiments, the polarized emission on elastic Rayleigh and Raman transitions to the $F=1$ lower level and inelastic Raman transitions to the $F=2$ level would need to be accounted for.

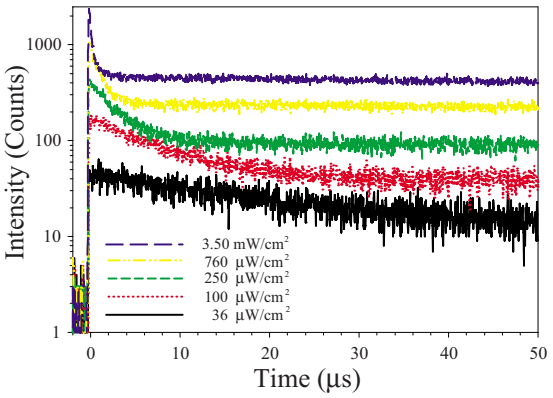

FIG. 3. (Color online) Dependence of the on-resonance transient fluorescence signals as the probe intensity is varied. The vertical organization of the data corresponds one to one with the intensities indicated in the figure legend.

In Fig. 3 we show results of measurements of the time evolution of the scattered light intensity for the probe laser tuned to $F=1 \rightarrow F'=0$ resonance transition. The measurements are made for a range of probe-laser intensities as shown. From Fig. 3, it is seen that both the peak and the steady-state scattered light intensities increase with increasing probe-laser intensity. We point out that the peak scattering rates as indicated in Fig. 3 are also consistent with the estimated scattering rates on this transition—as determined from the transition scattering cross section, the sample characteristics, and the overall detection efficiency. As shown in Fig. 4, the increase of the steady-state intensity is approximately linear for the lower intensity but indicates approach to the saturation for the highest probe intensity. Optical saturation is unexpected for the probe-laser intensities used in

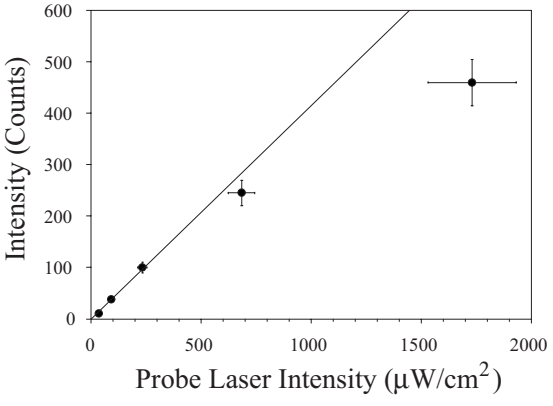

FIG. 4. Laser intensity dependence of the steady-state scattering signals for the on-resonance excitation of the ^{87}Rb $F=1 \rightarrow F'=0$ transition.

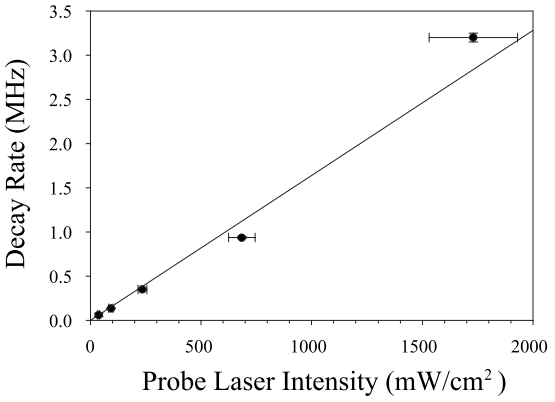

FIG. 5. Probe-laser intensity dependence of the exponential decay rate for the on-resonance excitation of the ^{87}Rb $F=1\rightarrow F'=0$ transition. The straight line is drawn to guide the eyes.

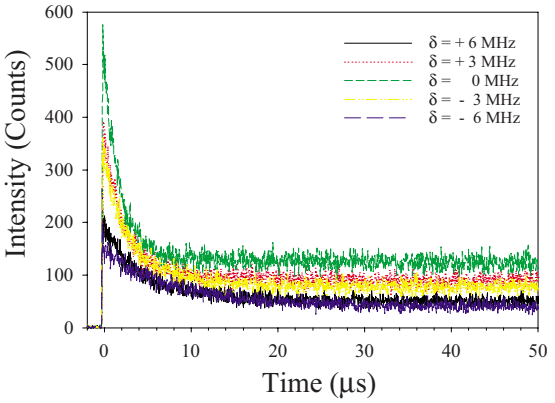

FIG. 6. (Color online) Detuning dependence of the probe fluorescence signals at a fixed probe-laser intensity of 350 μW/cm^2.

this set of results, for the on-resonance saturation intensity is $I_s=14.6$ mW/cm^2 for this transition. We believe that this lower intensity indication of saturation is due to the dominance of the optical pumping rate over that for replenishing the $F=1$, $m=0$ state by diffusive light-scattering, spontaneous emission, and spin precession due to background magnetic fields. Although a steady state between the various processes will always be reached, the amount of diffusive flux in the sample depends on the fraction of atoms in the $m=0$ ground level component both through the strength of the optical pumping process and through the resulting steady-state optical depth of the sample. Even though such an intensity-dependent behavior can occur due to other processes, such as optical heating or acceleration of the atoms out of the observation region, these effects are not expected to be important for the relatively short-time scales of the data in Fig. 3.

On the other hand, we observe that the measured intensity reaches a steady state for all probe-laser intensities used. As the steady-state intensity is proportional to the population in the $F=1$, $m=0$ state, we interpret this to mean that the optical pumping due to the probe laser reaches a balance with repumping processes due to multiply scattered light, atomic collisions, or precession of $m=\pm 1$ atoms into the $m=0$ state. For the conditions under which the measurements are made, atomic collisions are expected to negligibly effect the results. Spin precession can be caused either by residual uncompensated magnetic fields in the vicinity of the ultracold sample or due to transient fields due to the shutoff of the MOT quadrupole coils. On the time scale of the data in Fig. 3, the most likely competing process is the diffusely scattered light due to the significant optical thickness of the atomic sample.

It is also clear from Fig. 3 that the transient decay rates are qualitatively faster for higher probe intensity, while for longer times a steady state is reached. In fact, the decaying part of the transient response is very well represented by a single exponential form with a decay constant linearly dependent on the probe-laser intensity. These results are shown in Fig. 5. For the probe intensities used, the measured decay rates are consistent with estimates of the scattering rate of atoms out of the $F=1$, $m=0$ state.

In Fig. 6 we show the spectral variation in the probe fluorescence signals at approximately fixed probe-laser intensity. For these measurements, the probe intensity varies by a few percents during a given run. These differences are sufficient to account for the slight variations in the transient shape for equal positive and negative detunings. As expected, the transient becomes slower at greater detunings as the scattering cross section—and thus the optical pumping rate—is decreased. These results are thus consistent with our interpretation of the intensity and decay rates associated with the on-resonance transient signals.

B. Fluorescence measurements: Trap magnetic fields on

In this section, we turn to measurements made while the MOT quadrupole magnetic field is either left on during the fluorescence measurement phase or when it is turned off during the course of the measurement process.

To illustrate the overall effect, we present in Fig. 7 the result of the measurement of the time dependence of the scattered probe light signals for $\delta=0$ and at a fixed and weak probe-laser intensity of about 40 μW/cm^2. In this data, measurements with the MOT quadrupole field on and off are made after a delay of 500 μs. For the red curve, measurements are made with the MOT quadrupole field on continu-

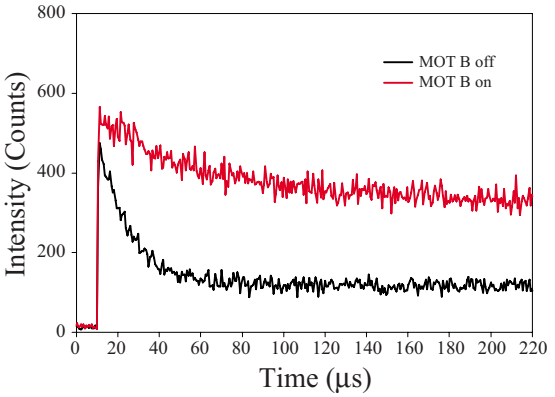

FIG. 7. (Color online) Comparison of probe-excited transient signals for the on-resonance excitation with the MOT quadrupole B field on (lighter curve) or off (darker curve). The probe-laser intensity is 40 μW/cm^2. These results should be compared with those of Fig. 3.

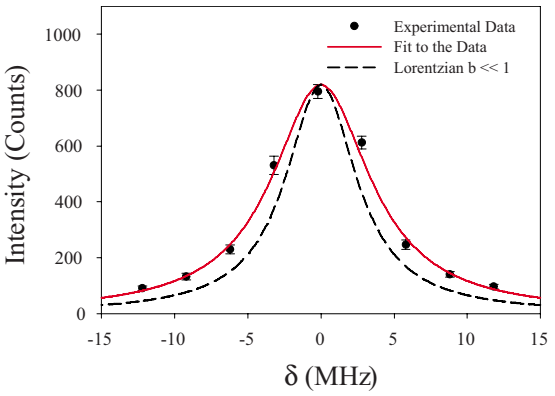

FIG. 8. (Color online) Spectral variation in the total scattered light intensity from the MOT. A fit to the data gives the indicated peak optical depth of about 3.5(5) for the $F=1\rightarrow F'=0$ transition. For comparison, the dashed black curve is a Lorentzian line shape with the expected detuning variation for an optically thin MOT with $b\ll 1$.

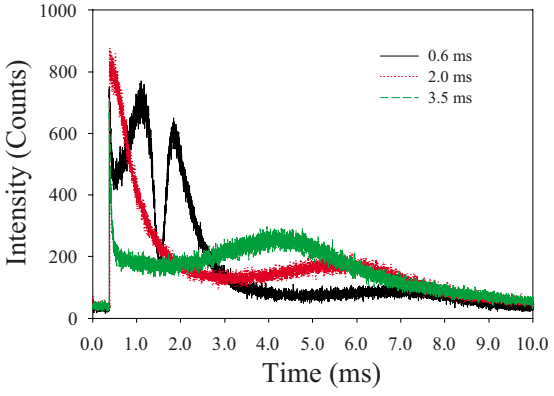

FIG. 9. (Color online) Time evolution of the probe fluorescence signal for different turn off times of the MOT quadrupole field relative to the probe turn on time origin.

ously. The modification of the size of the transient part of the signal and the steady-state level is clear. We interpret this result as follows. First, the optical pumping produces a spin quadrupole moment in the $F=1$ level as the atoms are pumped via quasielastic Raman scattering into the $m=\pm 1$ and $m=0$ states. Because for each scattering event the relative amplitudes in these states are coherent, the spin moments precess in any magnetic field present in the MOT environment. For B fields not sharing a common symmetry axis with the spin moments, some amplitude evolves from $m=\pm 1$ states into the $m=0$ state, where it can be accessed if the linearly polarized probe beam is on. As the Zeeman splitting in the $F=1$ level is about 700 kHz/G, the MOT quadrupole field of about 10 G/cm can have a large effect on the scattered light dynamics. With reference specifically to the data of Fig. 7, for any given atom in the sample, there should be coherent precession of the spins, leading to Zeeman beats in the probed $m=0$ amplitude. However, the MOT quadrupole field is spatially inhomogeneous and so there will be a distribution of precession frequencies which we expect will average out the beats in the total probe fluorescence signal that we observe.

To exploit these results, we obtained the detuning dependence of the peak-scattered light intensity. We expect that this quantity is dependent on the initial optical depth of the medium, as negligible optical pumping should occur for early times and lower probe intensity. These results are shown in Fig. 8 and are compared with the calculated variation in the amount of light scattered out of the coherent probe beam as a function of detuning, leaving the peak optical depth and overall signal amplitude as a fitting parameters. In the derivation of these expressions, a weak-field probe is assumed, and the total loss of light from the coherent beam is assumed to come from the scattering according to the Beer-Lambert law. This light is assumed to reappear in the form of single or multiply scattered radiation, which is reasonable for scattering from an ultracold atomic gas. Integrating over a Gaussian atom distribution and for an incident plane wave with average intensity I_0, the total scattered power $P(b)$ may be written exactly in terms of standard functions as

$$P(b) = 2\pi I_0 r_0^2[\mathrm{Ei}(b) - \gamma - \ln b]. \tag{3.1}$$

Here $\mathrm{Ei}(b)$ is the exponential integral and γ is the Euler-Mascheroni constant. Alternatively, it is useful for fitting purposes to express $P(b)$ in terms of the convergent series as an infinite summation,

$$P(b) = 2\pi I_o r_o^2 \sum_{n=1}^{\infty} (-1)^{n+1} \frac{b^n}{nn!} \tag{3.2}$$

$$b = b_0/[1 + (2\delta/\gamma)^2]. \tag{3.3}$$

Here I_o is the incident probe intensity assumed to be uniform over the cross section of the sample, while b_o is the peak optical depth given by Eq. (2.3). The result of a fit of the data to these equations is shown as the solid red curve in Fig. 8 for a peak optical depth of $b_o=3.5(5)$. The agreement is quite satisfactory. For comparison purposes, the limiting case of the relative scattering rate for very small optical depth b as a function of detuning is shown as the dashed black curve in Fig. 8. As guide for the eyes, this curve is normalized to the same peak intensity as the fit to the data. We point out that although the differences between the optically thin and measured scattering signal appear small at first sight, there is quite good sensitivity, particularly in the spectral wings of the resonance. For example, at a detuning of around +12 MHz, the measured intensity is twice what would be expected for an optically thin medium. To obtain such a larger scattering signal would require a spectral shift of about 4 MHz to smaller detunings. For this reason, the probe-laser full spectral width of less than 1 MHz was neglected in the fit to the data.

Finally, to further examine the role of the optical pumping suppression by an external and inhomogeneous magnetic field, we have made measurements of the scattered light intensity for time periods up to 10 ms after the MOT lasers and quadrupole field are shut off. The results of these experiments are shown in Fig. 9. We first point out that the atomic cloud expands significantly during the scale of the measurements, leading to a reduction in the number of atoms within

the field of view of the light collection optics. We thus expected and observed that the total intensity of the signals decreased significantly with time over a several milliseconds time period. The main point for our purposes here is that the strong temporal modulation of the signals is also seen in the several milliseconds time range of the data in Fig. 9. The shift in the relative starting time of the signals occurs because of the time origin shift of the probe fluorescence signal relative to different magnetic field turn off times. This shows that the beats are generated by the transient MOT magnetic field and not a steady field about which the atomic quadrupole could precess. The signals are proportional in each case to the number of atoms that are in the $m=0$ level at any given time. We believe that the time variation in the signals is due to the evolution of the induced fields generated when the MOT fields are shut off. The fields arise from induced currents in the MOT quadrupole coils, the MOT shim magnetic field coils, and eddy currents in the MOT chamber and other conducting or magnetizable materials in the vicinity of the apparatus. The effect is in general complicated but shows a strong sensitivity to quite small residual fields. For example, the longest beat time in the data is about 5 ms, which suggests an average magnetic field of around 50 μG. This field is decreasing in time, as is evidenced by the temporal decrease in the beat frequency with time. In order to examine the sensitivity limits of this effect, further and more controlled experiments are planned in both a MOT and an optical dipole trap environment (where hold times up to 10 s are possible in our apparatus).

IV. CONCLUSIONS

In summary, we have made measurements of near-resonance scattering of light from an ultracold sample of ^{87}Rb atoms on the $F=1\rightarrow F'=0$ hyperfine transition. The detuning and probe intensity dependences of the time-resolved scattered intensity show transients interpreted as due to the competition between Zeeman optical pumping in the lower-energy $F=1$ hyperfine level and diffuse light scattering in the optically deep sample. In addition, the role of Zeeman precession of the spin quadrupole moment in the MOT quadrupole field significantly effects the dynamics: both for long-time decays after the MOT magnetic field is turned off and on much shorter time scales if the fields are left on during the measurements. This observation leads to the possibility of detection of significantly smaller fields for the situation where the atom sample may be held for long periods of time in an optical dipole trap.

ACKNOWLEDGMENTS

We appreciate the financial support of the National Science Foundation (Grant No. NSF-PHY-0654226), the Russian Foundation for Basic Research (Grant No. RFBR-08-02-91355), and of INTAS (Project No. 7904).

[1] C. J. Pethick and H. Smith, *Bose-Einstein Condensation in Dilute Gases* (Cambridge University Press, Cambridge, UK, 2002).
[2] R. Wester, S. D. Kraft, M. Mudrich, M. U. Staudt, J. Lange, N. Vanhaecke, O. Dulieu, and M. Weidemüller, Appl. Phys. B: Lasers Opt. **79**, 993 (2004).
[3] R. M. Camacho, C. J. Broadbent, I. Ali-Khan, and J. C. Howell, Phys. Rev. Lett. **98**, 043902 (2007).
[4] D. Bouwmeester, A. Ekert, and A. Zeilinger, *The Physics of Quantum Information* (Springer-Verlag, Berlin, 2000).
[5] K. K. Ni, S. Ospelkaus, M. H. G. de Miranda, A. Pe'er, B. Neyenhuis, J. J. Kirbel, S. Kotochingova, P. S. Julienne, D. S. Jin, and J. Ye, Science **322**, 231 (2008).
[6] M. Vengalattore, J. M. Higbie, S. R. Leslie, J. Guzman, L. E. Sadler, and D. M. Stamper-Kurn, Phys. Rev. Lett. **98**, 200801 (2007).
[7] P. W. Anderson, Phys. Rev. **109**, 1492 (1958).
[8] V. S. Letokhov, Sov. Phys. JETP **26**, 835 (1968).
[9] H. Cao, Waves Random Media **13**, R1 (2003).
[10] E. Akkermans and G. Montambaux, *Mesoscopic Physics of Electrons and Photons* (Cambridge University Press, Cambridge, England, 2007).
[11] A. Gero and E. Akkermans, Phys. Rev. A **75**, 053413 (2007).
[12] W. Guerin, F. Michaud, and R. Kaiser, Phys. Rev. Lett. **101**, 093002 (2008).
[13] S. John, Phys. Rev. Lett. **53**, 2169 (1984).
[14] E. Yablonovitch, Phys. Rev. Lett. **58**, 2059 (1987).
[15] P. Sheng, *Introduction to Wave Scattering, Localization, and Mesoscopic Phenomena* (Academic, San Diego, 1995).
[16] A. Lagendijk and B. A. van Tiggelen, Phys. Rep. **270**, 143 (1996).
[17] D. S. Wiersma, P. Bartolini, Ad Lagendijk, and R. Righini, Nature (London) **390**, 671 (1997).
[18] A. A. Chabanov, M. Stoytchev, and A. Z. Genack, Nature (London) **404**, 850 (2000).
[19] M. Storzer, P. Gross, C. M. Aegerter, and G. Maret, Phys. Rev. Lett. **96**, 063904 (2006).
[20] C. M. Aegerter, M. Störzer, W. Bührer, S. Fiebig, and G. Maret, J. Mod. Opt. **54**, 2667 (2007).
[21] C. M. Aegerter, M. Störzer, S. Fiebig, W. Bührer, and G. Maret, J. Opt. Soc. Am. A **24**, A23 (2007).
[22] G. Labeyrie, F. de Tomasi, J. C. Bernard, C. A. Muller, C. Miniatura, and R. Kaiser, Phys. Rev. Lett. **83**, 5266 (1999).
[23] G. Labeyrie, R. Kaiser, and D. Delande, Appl. Phys. B: Lasers Opt. **81**, 1001 (2005).
[24] Mark D. Havey and Dmitriy V. Kupriyanov, Phys. Scr. **72**, C30 (2005).
[25] D. V. Kupriyanov, I. M. Sokolov, C. I. Sukenik, and M. D. Havey, Laser Phys. Lett. **3**, 223 (2006).
[26] E. Akkermans, A. Gero, and R. Kaiser, Phys. Rev. Lett. **101**, 103602 (2008).
[27] A. A. Golubentsev, Sov. Phys. JETP **59**, 26 (1984).
[28] R. Grimm, M. Weidemüller, and Yu. B. Ovchinnikov, Adv. At., Mol., Opt. Phys. **42**, 95 (2000).

[29] J. M. Choi, J. M. Kim, S. Y. Jeong, and D. Cho, J. Korean Phys. Soc. **46**, 425 (2005).

[30] Measurements on the same transition as studied here, but within the context of electromagnetically induced transparency, have been made by A. V. Durrant, H. X. Chen, S. A. Hopkins, and J. A. Vaccaro, Opt. Commun. **151**, 136 (1998).

[31] A more recent value for the natural width of this transition may be found in B. E. Schultz, H. Ming, G. A. Noble, and W. A. van Wijngaarden, Eur. Phys. J. D **48**, 171 (2008) Our measurements are made directly in MHz and are so reported in this paper.